

AUTHOR QUERY FORM

	<p>Journal: J. Appl. Phys. Article Number: 029928JAP</p>	<p>Please provide your responses and any corrections by annotating this PDF and uploading it to AIP's eProof website as detailed in the Welcome email.</p>
---	--	--

Dear Author,

Below are the queries associated with your article; please answer all of these queries before sending the proof back to AIP.

Article checklist: In order to ensure greater accuracy, please check the following and make all necessary corrections before returning your proof.

1. Is the title of your article accurate and spelled correctly?
2. Please check ations including spelling, completeness, and correct linking to authors.
3. Did you remember to include acknowledgment of funding, if required, and is it accurate? 

Location in article	Query / Remark: click on the Q link to navigate to the appropriate spot in the proof. There, insert your comments as a PDF annotation.
Q1	Please check that the author names are in the proper order and spelled correctly. Also, please ensure that each author's given and surnames have been correctly identified (given names are highlighted in red and surnames appear in blue).
Q2	Please reword the sentence beginning with "In the case studied here..." so that your meaning will be clear to the reader.
Q3	Please provide publisher's name for Ref. 14.
Q4	Figures must be cited in numerical order; therefore, we have renumbered Figs. 6, 4, 7, and 5 as 4, 5, 6, and 7. Please check.
	<p>Please confirm ORCIDs are accurate. If you wish to add an ORCID for any author that does not have one, you may do so now. For more information  about ORCID, see https://orcid.org/.</p> <p>Benjamin Vial-0000-0001-9468-0286 Yang Hao-0000-0002-9949-7226</p>
	<p>Please check and confirm the Funder(s) and Grant Reference Number(s) provided with your submission:</p> <p> Engineering and Physical Sciences Research Council, EP/P005578/1</p> <p>Please add any additional funding sources not stated above:</p>

Thank you for your assistance.

Enhanced tunability in ferroelectric composites through local field enhancement and the effect of disorder

3

4 Cite as: J. Appl. Phys. 126, 000000 (2019); doi: 10.1063/1.5101053

5 Submitted: 23 April 2019 · Accepted: 5 July 2019 ·

6 Published Online: ■■■ 2019

7 Benjamin Vial^{a)} and Yang Hao^{b)}

Q1

8 AFFILIATIONS

9 School of Engineering and Computer Science, Queen Mary, University of London, London E1 4NS, United Kingdom

10

11 ^{a)}Electronic mail: b.vial@qmul.ac.uk12 ^{b)}Electronic mail: y.hao@qmul.ac.uk

13

14 ABSTRACT

15 We investigate numerically the homogenized permittivities of composites made of low-index dielectric inclusions in a ferroelectric matrix
 16 under a static electric field. A refined model is used to take into account the coupling between the electrostatic problem and the electric field
 17 dependent permittivity of the ferroelectric material, leading to a local field enhancement and permittivity change in the ferroelectric.
 18 Periodic and pseudorandom structures in two dimensions are investigated, and we compute the effective permittivity, losses, electrically
 19 induced anisotropy, and tunability of these metamaterials. We show that the tunability of such composites might be substantially enhanced
 20 in the periodic case, whereas introducing disorder in the microstructure weakens the effect of the enhanced local permittivity change. Our
 21 results may be useful to guide the synthesis of novel composite ceramics with improved characteristics for controllable microwave devices.

22 © 2019 Author(s). All article content, except where otherwise noted, is licensed under a Creative Commons Attribution (CC BY) license
 23 (<http://creativecommons.org/licenses/by/4.0/>). <https://doi.org/10.1063/1.5101053>

24 I. INTRODUCTION

25 Ferroelectric materials play a crucial role in reconfigurable
 26 microwave devices with typical applications including antenna
 27 beam steering, phase shifters, tunable power splitters, filters,
 28 voltage controlled oscillators, and matching networks.¹ Both bulk
 29 ceramics and thin films have been employed to design frequency
 30 agile components^{2–4} and metamaterials.^{5,6} The main reason for
 31 using ferroelectric materials is their strong dependence of their
 32 permittivity ϵ on an applied electric field E , which is measured by
 33 their tunability defined as $n = \epsilon(0)/\epsilon(E)$, along with a nonhyste-
 34 resis behavior when used in their paraelectric state. The key
 35 requirements for antenna and microwave applications are large
 36 tunability and low losses. These two characteristics are correlated
 37 and one has to find a trade-off for optimal device performance,
 38 which can be quantified by the so-called commutation quality
 39 factor $K = (n - 1)^2 / (n \tan \delta(0) \tan \delta(E))$, where $\tan \delta$ is the loss
 40 tangent. These materials have usually high permittivity values
 41 even at microwave frequencies, often leading to slow response
 42 time and impedance mismatch, which can be an issue in some prac-
 43 tical applications. Thus, it has been considered to mix ferroelectric

44 ceramics with low-index and low-loss nontunable dielectrics in order
 45 to reduce both permittivity values and losses or to use porous ceram-
 46 ics to achieve the same goals without unwanted chemical reactions at
 47 the boundaries between dissimilar materials. In particular, the addi-
 48 tion of magnesium oxide in barium strontium titanate (BST) ceram-
 49 ics has been shown to decrease the losses while keeping good
 50 tunability.^{7,8} Ceramics such as Pb(Zr, Ti)O₃ (PZT) and BaTiO₃ (BT)
 51 have been used as fillers in polymer-based composites with high
 52 dielectric constant.⁹ Other mixtures include metal–polymer compos-
 53 ites¹⁰ and electroactive polymers such as poly(vinylidene fluoride)
 54 (PVDF) with high index dielectric inclusions.¹¹

55 The effective parameters of those composites have been
 56 investigated^{12–15} and it has been found that the permittivity can be
 57 greatly reduced while losses are much less sensitive to the dielectric
 58 phase addition and, in some situations, can lead to a small increase
 59 of the tunability of the mixtures. Analytical models based on the
 60 Bruggeman effective medium approach for low concentration of
 61 dielectrics were derived for different configurations (columnar,
 62 layered, and spherical inclusions models) and have been success-
 63 fully compared with numerical simulations and experiments.¹²

⁶⁴ In the context of porous ferroelectrics, the homogenized properties
⁶⁵ strongly depend on the size and morphology of the pores.^{16,17}
⁶⁶ Recently, the concept of tailoring the nonlinear properties of ferro-
⁶⁷ electric and dielectric structures by local field engineering has been
⁶⁸ introduced.^{18–20} It was shown through finite element calculation
⁶⁹ including the nonlinear coupling that, by employing composite
⁷⁰ materials made of linear dielectric inclusions into a ferroelectric
⁷¹ matrix, one can lower the permittivity while maintaining high tun-
⁷² ability, due to the local field in the ferroelectric phase that is tuned
⁷³ by the linear dielectric phase. Moreover, the effect of grain sizes in
⁷⁴ ferroelectric ceramics was studied using a model taking the field
⁷⁵ enhancement into account at the grain boundaries, and the pre-
⁷⁶ dicted behavior was successfully compared to experimental data.¹⁹
⁷⁷ Generally, there is a need for refined theoretical and numerical
⁷⁸ models to explain and design tunable materials and composites
⁷⁹ with tailored nonlinear properties. Note that the general method
⁸⁰ followed by our coupled model could be applied to other types of
⁸¹ tunable system where local field enhancement and amplification is
⁸² relevant, including ferromagnetic metamaterials,²¹ liquid crystals
⁸³ based devices,²² or field-enhanced carrier dynamics in doped semi-
⁸⁴ conductors at other frequency ranges, particularly in the terahertz
⁸⁵ and near-infrared.^{23,24}

⁸⁶ This study investigates numerically the effective permittivity of
⁸⁷ composites made of dielectric inclusions in a ferroelectric matrix
⁸⁸ by using a two-scale convergence method.^{25,26} The originality lies
⁸⁹ in the fact that a fully coupling model is employed to calculate the
⁹⁰ electrostatic field distribution when a uniform biasing field is
⁹¹ applied on the structures, which will result in a local modification
⁹² of the permittivity in the ferroelectric phase due to the micro-
⁹³ structure. As compared to a simple uncoupled model where the
⁹⁴ ferroelectric phase is only modified through the biasing field, the
⁹⁵ resulting effective permittivity, dielectric losses, tunability, and
⁹⁶ anisotropy significantly differ. In contrast with earlier studies in
⁹⁷ the literature,^{18,19} we account for the nonlinear coupling beyond
⁹⁸ the first iteration and use a two-scale convergence homogeniza-
⁹⁹ tion analysis to obtain the effective parameters at higher frequen-
¹⁰⁰ cies, instead of a capacitance-based model valid in the static
¹⁰¹ regime. This is an important point as, contrary to most homoge-
¹⁰² nization procedures that are based on a quasistatic approximation,
¹⁰³ the two-scale convergence method fixes the frequency and lets the
¹⁰⁴ characteristic size of the system (the periodicity of the compos-
¹⁰⁵ ites) tend to zero.²⁶ This asymptotic analysis allows one to study
¹⁰⁶ the frequency dependence of the effective parameters. In addition,
¹⁰⁷ analytical models for the effective permittivity routinely employed
¹⁰⁸ in the literature, such as Maxwell-Garnett or Bruggeman theories,
¹⁰⁹ are limited to a few canonical shapes of the inclusions and cannot
¹¹⁰ handle arbitrary geometries and media with spatially varying
¹¹¹ properties. This last point is of particular importance in the
¹¹² context of this study since we have to account for the field
¹¹³ induced local permittivity change.

¹¹⁴ The model we developed has been implemented with the
¹¹⁵ finite element method (FEM), and we realize a systematic compu-
¹¹⁶ tational study of ferroelectric-dielectric mixtures. First, we consider
¹¹⁷ metamaterials consisting of a square array of parallel dielectric
¹¹⁸ rods with circular cross section in a ferroelectric host and then
¹¹⁹ investigate the effect of random distribution of those rods within
¹²⁰ the unit cell.

II. THEORY AND NUMERICAL MODEL

121

We consider a composite made of a ferroelectric material¹²² with anisotropic permittivity $\epsilon^f(E)$ that is dependent on an¹²³ applied electric field E and a nontunable dielectric of permittivity¹²⁴ ϵ^d , which are both nonmagnetic. The structures under study are¹²⁵ invariant along the z direction, which leads to the standard¹²⁶ decomposition of the wave equation in the transverse electric case¹²⁷ (TE, electric field parallel to the direction of invariance) and the¹²⁸ transverse magnetic case (TM, magnetic field parallel to the¹²⁹ direction of invariance). A uniform biasing field is applied in¹³⁰ order to be able to tune the effective permittivity. Modeling¹³¹ homogenized properties of this type of mixtures can be done by¹³² assuming that the electric field distribution is uniform through-¹³³ out the sample so that the study of the tunability is essentially¹³⁴ achieved by changing the value of the properties in the ferroelec-¹³⁵ tric phase and computing the effective permittivity of the com-¹³⁶ posite. We refer to this approach as the uncoupled model in the¹³⁷ following. However, a more accurate description is to take into¹³⁸ account the change of the electric field by the microstructure, if¹³⁹ any. We, therefore, need to solve an electrostatic equation to find¹⁴⁰ the field distribution within the material, but its solution depends¹⁴¹ on the permittivities of both materials, and the permittivity in the¹⁴² ferroelectric phase depends on this induced electric field: this¹⁴³ leads to a strongly coupled problem.¹⁴⁴

A. Permittivity model

145

We use barium strontium titanate (BST) as our ferroelectric¹⁴⁶ material. $Ba_xSr_{1-x}TiO_3$ samples were fabricated using the conven-¹⁴⁷ tional sintering method with a barium ratio of $x = 0.6$ to obtain a¹⁴⁸ dielectrically tunable material as reported in the literature.^{11,27}¹⁴⁹ The tunability was measured using an impedance analyzer up to¹⁵⁰ 100 MHz and at 3.8 GHz using a loaded microstrip split ring reso-¹⁵¹ nator.²⁸ The measured tunability of the in-house BST samples of¹⁵² 27% under 1 kV/mm DC bias was in agreement with those¹⁵³ reported elsewhere.^{11,27} The method presented is, however,¹⁵⁴ general and relies only on the gradient of the dielectric tunability¹⁵⁵ vs electric field and could be applied to any tunable host material.¹⁵⁶ The normalized permittivity value as a function of biasing field is¹⁵⁷ reported in Fig. 1.¹⁵⁸

To describe the permittivity, we make use of the Landau¹⁵⁹ potential given by $F(P, E) = F_0 + aP^2/2 + bP^4/4 + cP^6/6 - EP$,¹⁶⁰ where E is the applied electric field and P is the polarization.^{29,30}¹⁶¹ Variations of the permittivity with the temperature can be taken¹⁶² into account through the coefficients a , b , and c , but we assume¹⁶³ that we are working at a constant room temperature. We further¹⁶⁴ assume that the material is not subject to any stress so that the vari-¹⁶⁵ ation of permittivity due to mechanical constraints is irrelevant.¹⁶⁶ The equation of state¹⁶⁷

$$\frac{\partial F(P, E)}{\partial P} = aP_0 + bP_0^3 + cP_0^5 - E = 0$$

gives the dependence of the polarization on the applied electric¹⁶⁸ field, with P_0 being the equilibrium polarization. Along the direc-¹⁶⁹ tion of a uniform applied electric field, the relative permittivity is¹⁷⁰

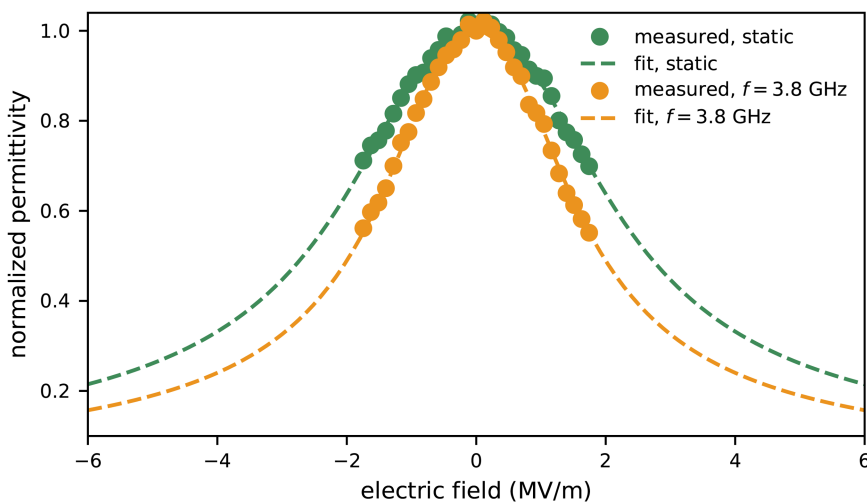


FIG. 1. Variation of the ferroelectric permittivity as a function of the applied electric field [dots: measurements; dashed lines: fit to formula (1)], for the static case (green) and at microwave frequencies (orange, $f = 3.8$ GHz). The fitting parameters are given in Table I.

171 given by

$$\boldsymbol{\epsilon}^f(E) = \left[\frac{\partial^2 F(P, E)}{\partial P^2} \right]^{-1} = \frac{\epsilon^f(0)}{1 + \alpha P_0^2 + \beta P_0^4}, \quad (1)$$

172 where $\epsilon^f(0) = 1/a$, $\alpha = 3b/a$, and $\beta = 5c/a$. The fitting parameters are given in Table I. As the norm of the field increases, the 173 permittivity decreases with a characteristic bell curve typical for a 174 ferroelectric material in its paraelectric state. Furthermore, assuming 175 that the crystalline principal axes of the ferroelectric material 176 are oriented in the coordinate directions and that the diagonal 177 components of the permittivity tensor are only function of the cor- 178 responding bias electric field components,³¹ we have 179

$$\boldsymbol{\epsilon}^f(E) = \begin{pmatrix} \epsilon_{xx}^f(E_x) & 0 & 0 \\ 0 & \epsilon_{yy}^f(E_y) & 0 \\ 0 & 0 & \epsilon_{zz}^f(E_z) \end{pmatrix}, \quad (2)$$

180 where each of the diagonal components has the functional form 181 given by Eq. (1). Note that we will use the static values of permittivity 182 for the electrostatic modeling, while we are interested in the 183 homogenized values of permittivity at microwaves.

B. Electrostatic model

185 The composites under study are made of two materials, thus 186 their permittivity is represented by a piecewise defined tensor 187 $\boldsymbol{\epsilon}(r, E)$, which is equal to $\boldsymbol{\epsilon}^f(E(r))$ in the ferroelectric phase and 188 $\text{diag}(\boldsymbol{\epsilon}^d)$ in the dielectric phase. In the following, we consider two

different cases for the biasing field. Because of the form (2) assumed for the ferroelectric permittivity tensor, ϵ_{zz} will not be changing for a field in the plane orthogonal to the z axis. This is the only component being relevant for TE polarization, so we consider in this case a uniform biasing electric field applied along the direction of invariance $E_0 = E_0 \mathbf{e}_z$. On the other hand, the in-plane components of $\boldsymbol{\epsilon}^f$ are tuned by E_x and E_y , therefore, without loss of generality, we consider a uniform applied electric field directed along the x axis $E_0 = E_0 \mathbf{e}_x$ for the TM polarization case. To calculate the total electric field in the material, one has to solve for the potential V satisfying Gauss' law

$$\nabla \cdot (\boldsymbol{\epsilon} \nabla V) = 0. \quad (3)$$

Note that for the TE case, the solution is trivial since the structures are invariant along z so that the electric field is equal to the uniform biasing field, and we will thus not study it in the following. However, in the TM case, the situation is much more complex: this is a coupled problem since the electric field $\mathbf{E} = -\nabla V$ derived from the solution of Eq. (3) depends on the permittivity distribution, which itself depends on the electric field. The coupled system formed of Eqs. (2) and (3) is solved iteratively until there is convergence on the norm of the electric field. Here, we would like to emphasize that the permittivity in the ferroelectric material, although uniform initially, is spatially varying due to the nonuniform distribution of the total electric field.

C. Homogenization

When the period of the composite metamaterial is much smaller than the wavelength, one can describe the properties of the composite by a bulk medium with homogenized parameters. The effective permittivity for TM polarization is calculated using a two-scale convergence homogenization technique.^{25,26} For this purpose, one has to find the solutions ψ_j of two annex problems $\mathcal{P}_j, j = \{1, 2\}$,

$$\nabla \cdot [\xi \nabla (\psi_j + r_j)] = 0, \quad (4)$$

TABLE I. Fitting parameters to model (1) for the measured permittivity values as a function of applied electric field shown in Fig. 1.

Case	$\epsilon^f(0)$	$\alpha (\mu\text{m}^2/\text{V}^2)$	$\beta (\mu\text{m}^4/\text{V}^4)$
Static	3050	0.120	0.024
$f = 3.8$ GHz	165	0.240	0.079

where $\mathbf{r} = (x, y)^T$ is the position vector in the xy plane and $\xi = \boldsymbol{\varepsilon}^T / \det(\boldsymbol{\varepsilon})$. The homogenized tensor $\tilde{\xi}$ is obtained with

$$\tilde{\xi} = \langle \xi \rangle + \boldsymbol{\phi}, \quad (5)$$

where $\langle \cdot \rangle$ denotes the mean value over the unit cell. The elements of the matrix $\boldsymbol{\phi}$ represent correction terms and are given by $\phi_{ij} = \langle \xi \nabla \psi_i \rangle_j$. Finally, the effective permittivity tensor can be calculated using $\tilde{\boldsymbol{\varepsilon}} = \tilde{\xi}^T / \det(\tilde{\xi})$.

Note that the TE case, which we shall not study here as no coupling happens, is trivial since the homogenized permittivity is simply the average of the permittivity in the unit cell: $\tilde{\boldsymbol{\varepsilon}} = \langle \boldsymbol{\varepsilon} \rangle$.

III. NUMERICAL RESULTS

In the following numerical results, the dielectric phase is supposed to be lossless and nondispersive with $\epsilon^d = 3$, while the ferroelectric material follows the permittivity described in Sec. II A and has a constant loss tangent, $\tan \delta^f = 10^{-2}$. Equations (3) and (4) are solved with a finite element method using the open source packages Gmsh³² and GetDP.³³ In both cases, we use a square unit cell Ω of length d with periodic boundary conditions along x and y . Second order Lagrange elements are used, and the solution is computed with a direct solver (MUMPS³⁴).

A. Two dimensional periodic metamaterial

Let us now consider a periodic square array of infinitely long dielectric rods of a circular cross section of radius r embedded in a ferroelectric matrix.

We first study the convergence of the coupled problem on the particular case with dielectric filling fraction $f = \pi r^2 / d^2 = 0.5$ and $E_0 = 2 \text{ MV/m}$. Figures 2(a) and 2(b) show the convergence of the real part and loss tangent of the components of the homogenized permittivity tensor, respectively. The yy components converge quickly and are almost unaffected by the coupling process, whereas the xx components change substantially from the initial conditions. This is due to the effect of the redistribution of the electrostatic field within the unit cell [see Figs. 2(c) and 2(d)], where the x component of the electric field is still much stronger than the y component, even if spatially varying in the ferroelectric medium. At equilibrium, the electric field is concentrated close to the y axis in between two neighboring rods. This, in turn, affects the permittivity distribution [see Figs. 2(e) and 2(f)] and the homogenized properties of the composite.

We computed the effective parameters of these metamaterial structures for different radii of the rods and studied their behavior when subjected to an external electrostatic field (see Fig. 3). The results of our coupled model differ significantly from the uncoupled one. Increasing the dielectric fraction lowers the effective permittivity, while the losses are slightly reduced but much less

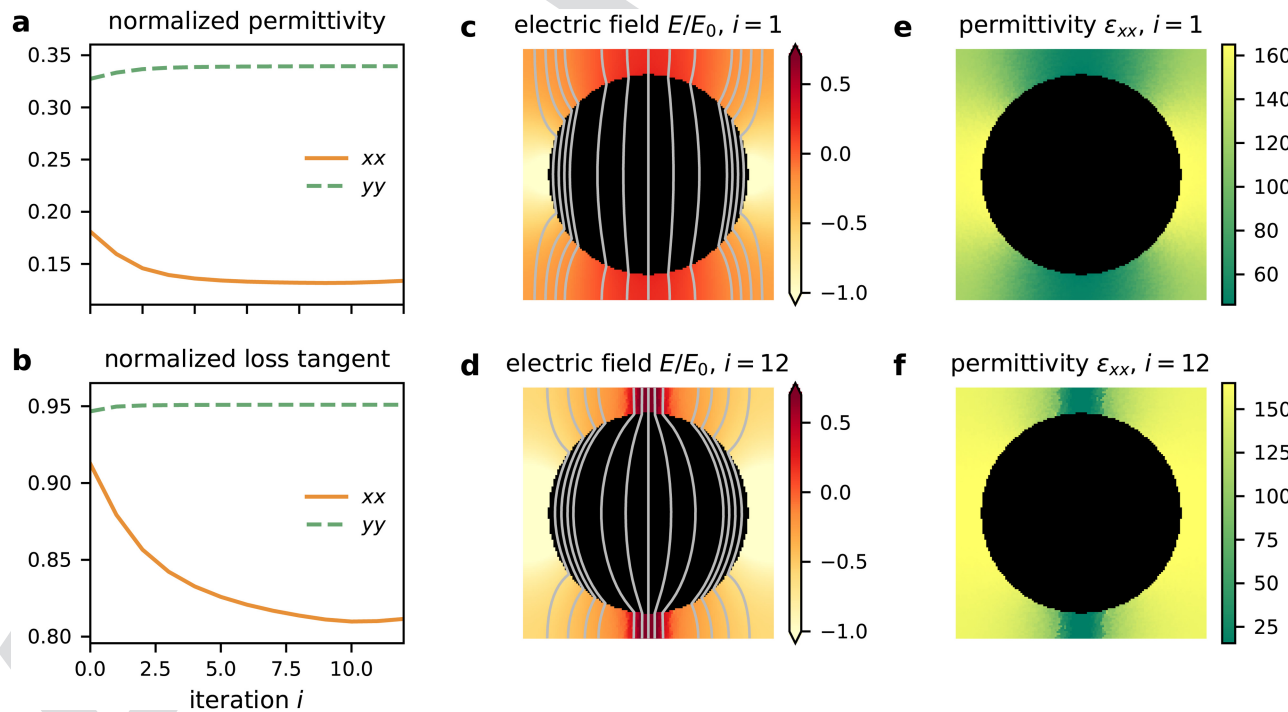


FIG. 2. Convergence of the coupled problem. Real part (a) and loss tangent (b) of the components of the homogenized permittivity tensor as a function of iteration step i . The values are normalized to the corresponding quantities for the bulk ferroelectric material. The distribution of the normalized electric field (color map: magnitude in the logarithmic scale; lines: equipotential contours) and of the xx component of the permittivity tensor is shown for $i = 1$ [(c) and (d)] and $i = 12$ [(e) and (f)].

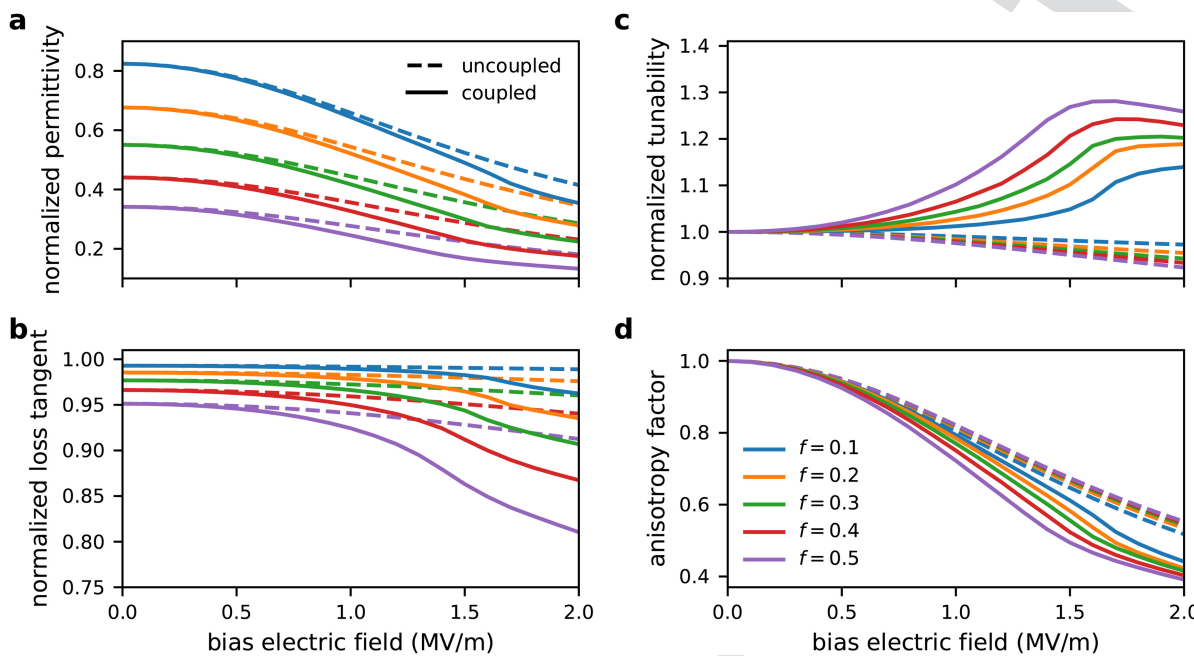


FIG. 3. Effective parameters of the 2D metamaterials as a function of the applied electric field for various filling fraction of dielectric. (a) Normalized permittivity, (b) normalized loss tangent, (c) normalized tunability, and (d) anisotropy factor. The solid lines correspond to the coupled model, and the dashed lines to the uncoupled model. The values are normalized to the corresponding quantities for the bulk ferroelectric material.

sensitive. Due to the inhomogeneous redistribution of the permittivity over the ferroelectric domain, the overall tunability changes. In the case studied here, taking into account the coupling leads to an effective tunability increase with higher dielectric concentration, and that is larger than the tunability of bulk ferroelectric. This can be seen in Fig. 3(c), where we plot the tunability of the composites along the x axis, $\tilde{n}(E) = \tilde{\epsilon}_{xx}(E)/\tilde{\epsilon}_{xx}(0)$, normalized to the tunability of the bulk ferroelectric $n(E) = \epsilon_{xx}^f(E)/\epsilon_{xx}^f(0)$. Two concurrent effects are at stake here: on the one hand, the dilution of ferroelectric makes the composite less tunable, but on the other hand, the rearrangement of the electrostatic field surrounding the inclusion

and its concentration in some region will cause a higher permittivity change locally. The relative strength of those phenomena is governed by the shape of the inclusion and its permittivity, and so, it is envisioned that the performance of the composites might be enhanced by engineering their microstructure. Those observations are consistent with previously published numerical and experimental results¹⁸ where the local field enhancement in porous ferroelectrics has been shown to possibly increase tunability with reducing permittivity for small porosity levels. Our approach also agrees with an analytical spherical inclusion model predicting an increase of the tunability with the dilution of the ferroelectric.¹²

Random material samples, $f = 0.5$

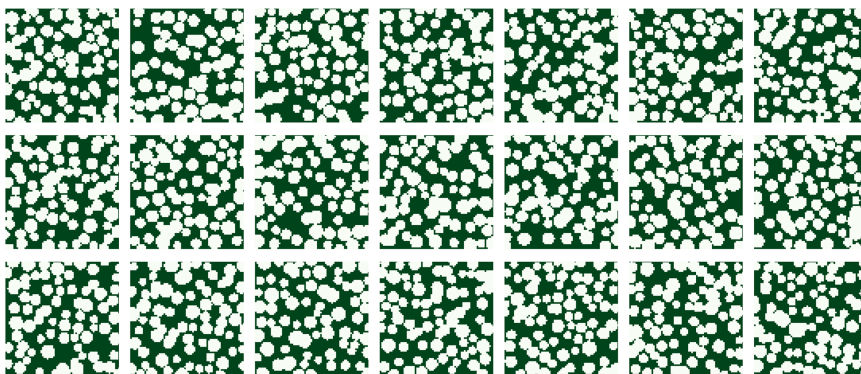


FIG. 4. Permittivity distribution of the numerical samples used for $f = 0.5$. The dark color indicates the ferroelectric material, while the light color represents the dielectric inclusions.

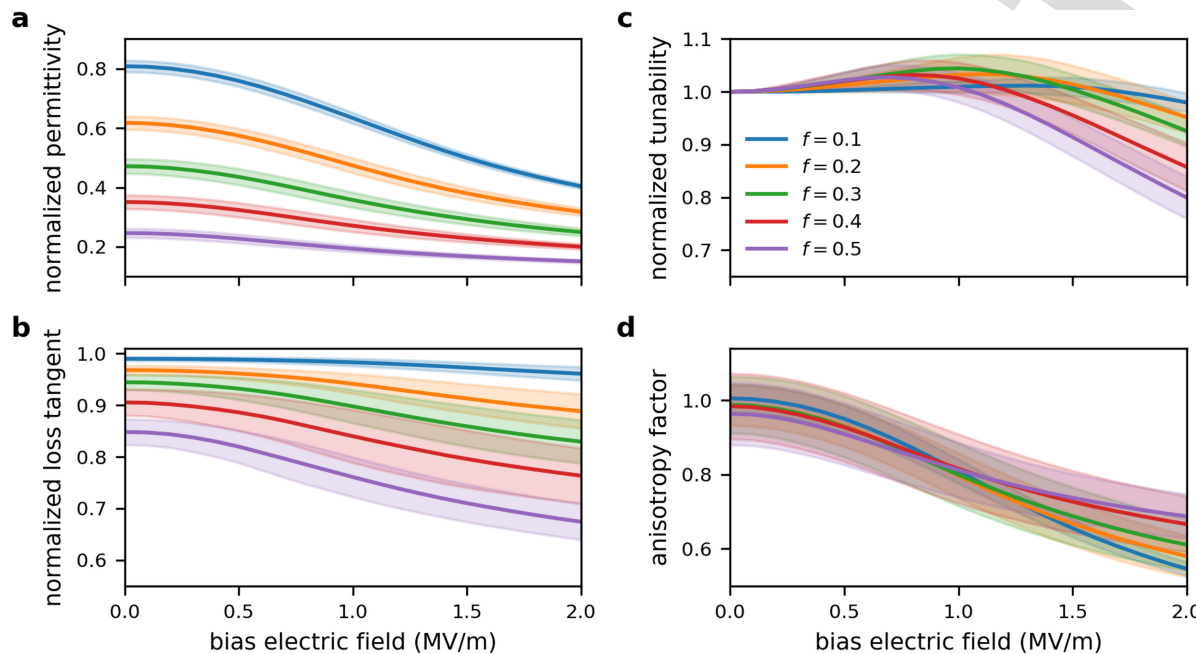


FIG. 5. Effective parameters of the pseudorandom composites as a function of the applied electric field for various filling fraction of dielectric, when the coupling is taken into account. (a) Normalized permittivity, (b) normalized loss tangent, (c) normalized tunability, and (d) anisotropy factor. The solid lines represent the average values over the 21 samples, and the lighter error bands show a confidence interval corresponding to the standard deviation. The values are normalized to the corresponding quantities for the bulk ferroelectric material.

Q4

The geometry of the unit cell is symmetric so the homogenized material is isotropic when no field is applied. But when the sample is biased, the permittivity distribution becomes asymmetric due to the inhomogeneity of the electric field, thus making the effective material properties anisotropic. This geometric effect is added to the anisotropy arising from the material properties of the ferroelectric phase itself and depending on the topology and permittivity of the rods, one effect would be predominant. In the case studied here, the equilibrium permittivity distribution varies strongly along the bias direction and much less orthogonally to it, which adds anisotropy by diminishing the effective permittivity in the x direction. This local field induced effect is what makes the anisotropy stronger in our coupled model compared to the uncoupled one [cf. Fig. 3(d)], where we plot the anisotropy factor $\alpha = \epsilon_{xx}/\epsilon_{yy}$. Those subtle phenomena can only be rigorously taken into account by employing a coupling formalism and are responsible for the difference observed when compared to a simple uncoupled model.

306 B. Pseudorandom case

307 We finally study the effect of random distribution of the 308 inclusions within the unit cell on the effective parameters of the 309 composites. This is an important point as fabrication of randomly 310 dispersed inclusions is much more easy from a technological 311 perspective. For each filling fraction of the dielectric, we generated

21 numerical samples with inclusions of circular cross section of 312 average radius $r = d/20$ that can vary by $\pm 30\%$. Their center is 313 chosen randomly and the rods are allowed to overlap. An example 314 of distribution for $f = 0.5$ is given in Fig. 4. The effective material 315 properties are plotted in Fig. 5. Similar to the periodic case, the 316 permittivity decreases with increasing dilution of ferroelectric, 317 but for identical filling fraction, the permittivity is lower as com- 318 pared to the periodic array, and the smaller the dielectric concen- 319 tration, the larger is the difference. Losses decrease as well and 320 the reduction is substantially larger than the periodic case, with 321 higher variation from sample to sample as f increases. The effective 322 tunability is on average smaller than that in the periodic case, and 323 for low biasing fields and for some particular samples, it can be 324 greater than the bulk tunability. However, at higher applied electric 325 fields, normalized tunability becomes smaller than unity and is 326 reduced as one adds more dielectric. For comparison, the homoge- 327 nized parameters are plotted in Fig. 6 in the case where the coupling 328 is neglected. One can see that the coupled and uncoupled models 329 give similar results for the tunability, whereas the losses are still 330 smaller for the coupled case at higher fields.

331 The redistribution of electric field, permittivity, and conver- 332 gence of the effective parameters are displayed in Fig. 7. The effect 333 of disorder plays an important role here: the electrostatic field gets 334 concentrated in between neighboring inclusions and the smaller 335 the gap, the higher the field, hence a greater local permittivity 336 change. In addition, even if the distribution is random, one expects 337

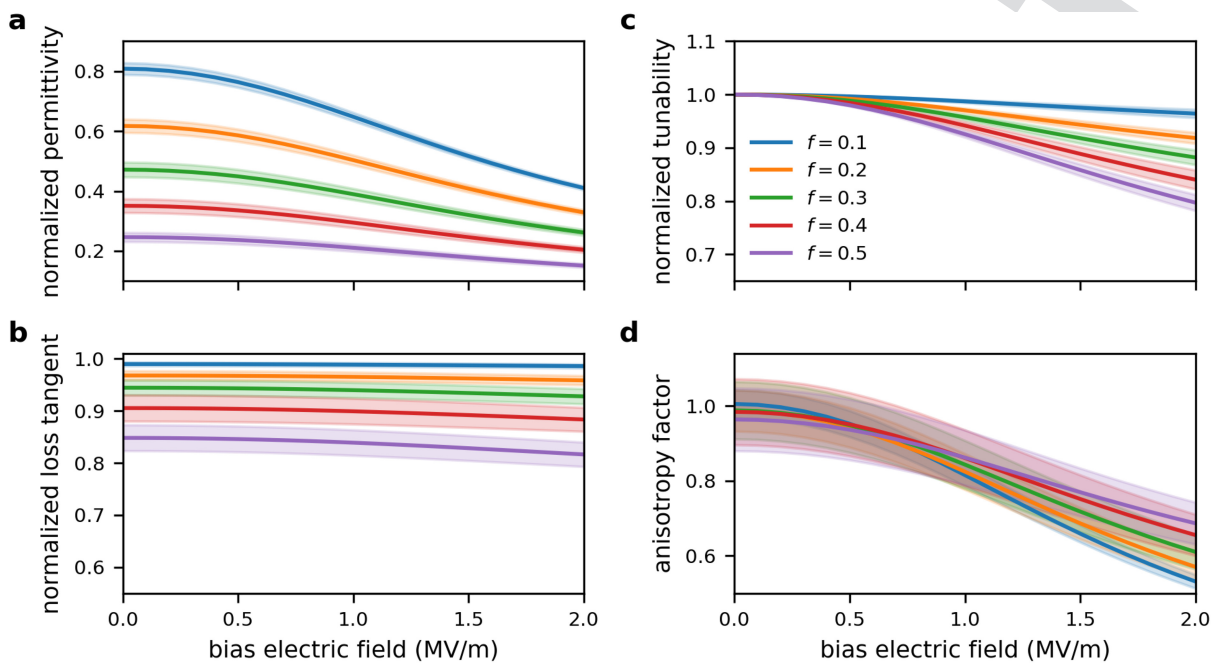


FIG. 6. Effective parameters of the random 2D mixtures as a function of the applied electric field for various filling fraction of dielectric, when the coupling is neglected. (a) Normalized permittivity, (b) normalized loss tangent, (c) normalized tunability, and (d) anisotropy factor. The solid lines represent the average values over the 21 samples, and the lighter error bands show a confidence interval corresponding to the standard deviation. The values are normalized to the corresponding quantities for the bulk ferroelectric material.

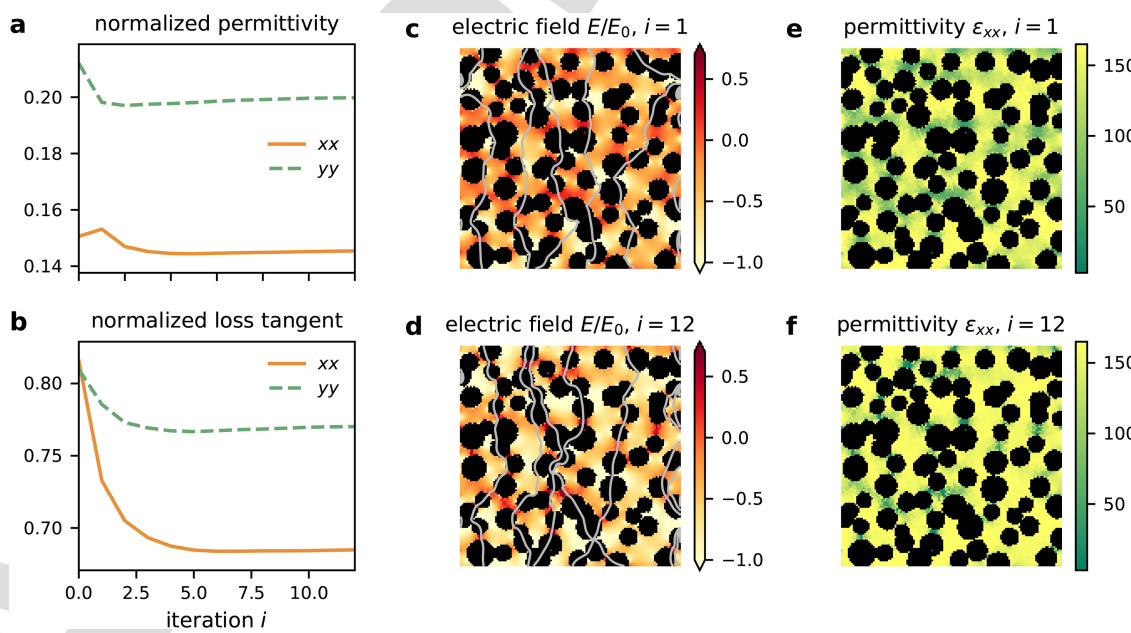


FIG. 7. Convergence of the coupled problem in the random case for one sample. Real part (a) and loss tangent (b) of the components of the homogenized permittivity tensor as a function of iteration step i . The values are normalized to the corresponding quantities for the bulk ferroelectric material. The distribution of the normalized electric field (color map: magnitude in the logarithmic scale, lines: equipotential contours) and of the xx component of the permittivity tensor is shown for $i = 1$ [(c) and (d)] and $i = 12$ [(e) and (f)].

338 that the anisotropy due to geometry would cancel for a sufficiently
 339 large number of rods (which is the case as the mean anisotropy
 340 factor is close to 1 when no bias field is applied). However, the
 341 anisotropy due to ferroelectric properties is important in this case
 342 as well, as both the x and y components of the electrostatic field are
 343 playing a role. Because of the relative positions of the rods, both ϵ_{xx}
 344 and ϵ_{yy} are affected by the coupling so that the anisotropy factor
 345 for higher fields is reduced as compared to the periodic case.
 346 However, even if there is a substantial variability from sample to
 347 sample, on average, the anisotropy factor decreases with increasing
 348 dielectric concentration.

349 IV. CONCLUSION

350 We have studied the homogenized properties of dielectric/
 351 ferroelectric mixtures using a rigorous model that takes into
 352 account the coupling between the electrostatic field distribution
 353 and the field dependent ferroelectric permittivity tensor. After
 354 convergence of the coupled problem, the effective permittivity
 355 tensor is calculated using a two-scale convergence homogenization
 356 theory. The results obtained by this model differ significantly
 357 from a simple assumption that the permittivity of the ferroelectric
 358 responds just to the uniform biasing field. We have considered
 359 both periodic and random arrays of dielectric rods in a ferroelec-
 360 tric matrix in 2D and studied their effective properties for TM
 361 polarization as a function of dielectric concentration and bias
 362 field. Importantly, adding more low index and low loss dielectric
 363 allows to decrease the overall permittivity significantly and
 364 slightly lower the losses. For the periodic case, the tunability is
 365 higher than the bulk due to local field enhancement, whereas this
 366 effect is strongly suppressed when the disorder is introduced. The
 367 asymmetric redistribution of the permittivity induces an effective
 368 anisotropy that is added to the one arising purely from the ferro-
 369 electric material. The properties of the composites are affected by
 370 multiple factors: geometry and the spatially dependent electric
 371 field that will induce locally a tunable, anisotropic response in the
 372 ferroelectric phase depending on its amplitude and direction.
 373 This suggests that the performances of the composites may be
 374 enhanced by distributing the two phases in an optimal way to get
 375 high tunability and low losses. Further work in that direction is
 376 needed as well as extending this study to 3D media. Finally,
 377 because the permittivity of the dielectric is much smaller than the
 378 ferroelectric one, it would be of great interest to use high contrast
 379 homogenization theory^{35,36} to study these kinds of mixtures. This
 380 would reveal the frequency dependent artificial magnetism due to
 381 "microresonances" in the high index phase and potentially lead to
 382 composites with tunable effective permeability.

383 ACKNOWLEDGMENTS

384 This work was funded by the Engineering and Physical
 385 Sciences Research Council (EPSRC), UK, under a grant (No. EP/
 386 P005578/1) "Adaptive Tools for Electromagnetics and Materials
 387 Modelling to Bridge the Gap between Design and Manufacturing
 388 (AOTOMAT)."

389 The authors would like to thank Henry Giddens for performing
 390 the measurements of ferroelectric permittivity used in this paper.

The codes necessary to reproduce the results in this article are 391
 freely available online at this address: <https://www.github.com/benivial/ferromtm>. 392 393

REFERENCES

- ¹A. K. Tagantsev, V. O. Sherman, K. F. Astafiev, J. Venkatesh, and N. Setter, "Ferroelectric materials for microwave tunable applications," *J. Electroceram.* **11**, 5–66 (2018).
- ²O. Vendik, E. Hollmann, A. Kozyrev, and A. Prudan, "Ferroelectric tuning of planar and bulk microwave devices," *J. Supercond.* **12**, 325–338 (1999).
- ³M. Lancaster, J. Powell, and A. Porch, "Thin-film ferroelectric microwave devices," *Supercond. Sci. Technol.* **11**, 1323 (1998).
- ⁴X. Xi, H.-C. Li, W. Si, A. Sirenko, I. Akimov, J. Fox, A. Clark, and J. Hao, "Oxide thin films for tunable microwave devices," *J. Electroceram.* **4**, 393–405 (2000).
- ⁵T. H. Hand and S. A. Cummer, "Frequency tunable electromagnetic metamaterial using ferroelectric loaded split rings," *J. Appl. Phys.* **103**, 066105 (2008).
- ⁶H. Zhao, L. Kang, J. Zhou, Q. Zhao, L. Li, L. Peng, and Y. Bai, "Experimental demonstration of tunable negative phase velocity and negative refraction in a ferromagnetic/ferroelectric composite metamaterial," *Appl. Phys. Lett.* **93**, 201106 (2008).
- ⁷P. Irvin, J. Levy, R. Guo, and A. Bhalla, "Three-dimensional polarization imaging of (Ba, Sr)TiO₃:MgO composites," *Appl. Phys. Lett.* **86**, 042903 (2005).
- ⁸U.-C. Chung, C. Elissalde, M. Maglione, C. Estournès, M. Paté, and J. P. Ganne, "Low-losses, highly tunable Ba_{0.6}Sr_{0.4}TiO₃/MgO composite," *Appl. Phys. Lett.* **92**, 042902 (2008).
- ⁹B. Wang, L. Luo, F. Ni, P. Du, W. Li, and H. Chen, "Piezoelectric and ferroelectric properties of (Bi_{1-x}Na_{0.8}K_{0.2}La_x)_{0.5}TiO₃ lead-free ceramics," *J. Alloys Compd.* **526**, 79–84 (2012).
- ¹⁰X. Li, Y.-F. Lim, K. Yao, F. E. H. Tay, and K. H. Seah, "Ferroelectric poly(vinylidene fluoride) homopolymer nanotubes derived from solution in anodic alumina membrane template," *Chem. Mater.* **25**, 524–529 (2013).
- ¹¹G. Hu, F. Gao, J. Kong, S. Yang, Q. Zhang, Z. Liu, Y. Zhang, and H. Sun, "Preparation and dielectric properties of poly(vinylidene fluoride)/Ba_{0.6}Sr_{0.4}TiO₃ composites," *J. Alloys Compd.* **619**, 686–692 (2015).
- ¹²V. O. Sherman, A. K. Tagantsev, N. Setter, D. Iddles, and T. Price, "Ferroelectric-dielectric tunable composites," *J. Appl. Phys.* **99**, 074104 (2006).
- ¹³L. Jylha and A. H. Sihvo, "Tunability of granular ferroelectric dielectric composites," *Prog. Electromagn. Res.* **78**, 189–207 (2008).
- ¹⁴V. O. Sherman, A. K. Tagantsev, and N. Setter, "Tunability and loss of the ferroelectric-dielectric composites," in *14th IEEE International Symposium on Applications of Ferroelectrics, ISAF-04, 2004* (■, 2004), pp. 33–38.
- ¹⁵K. F. Astafiev, V. O. Sherman, A. K. Tagantsev, and N. Setter, "Can the addition of a dielectric improve the figure of merit of a tunable material?," *J. Eur. Ceram. Soc.* **23**, 2381–2386 (2003).
- ¹⁶K. Okazaki and K. Nagata, "Effects of grain size and porosity on electrical and optical properties of PLZT ceramics," *J. Am. Ceram. Soc.* **56**, 82–86 (1973).
- ¹⁷R. Stanculescu, C. E. Ciomaga, L. Padurariu, P. Galizia, N. Horchidan, C. Capiani, C. Galassi, and L. Mitoseriu, "Study of the role of porosity on the functional properties of (Ba, Sr)TiO₃ ceramics," *J. Alloys Compd.* **643**, 79–87 (2015).
- ¹⁸L. Padurariu, L. Curecheriu, C. Galassi, and L. Mitoseriu, "Tailoring non-linear dielectric properties by local field engineering in anisotropic porous ferroelectric structures," *Appl. Phys. Lett.* **100**, 252905 (2012).
- ¹⁹L. Padurariu, L. Curecheriu, V. Buscaglia, and L. Mitoseriu, "Field-dependent permittivity in nanostructured BaTiO₃ ceramics: Modeling and experimental verification," *Phys. Rev. B* **85**, 224111 (2012).

- ⁴⁵¹ ²⁰A. Cazacu, L. Curecheriu, A. Neagu, L. Padurariu, A. Cernescu, I. Lisiecki, and
⁴⁵² L. Mitoseriu, "Tunable gold-chitosan nanocomposites by local field engineering,"
⁴⁵³ *Appl. Phys. Lett.* **102**, 222903 (2013).
- ⁴⁵⁴ ²¹L. Carignan, A. Yelon, D. Menard, and C. Caloz, "Ferromagnetic nanowire
⁴⁵⁵ metamaterials: Theory and applications," *IEEE Trans. Microw. Theory Techn.*
⁴⁵⁶ **59**, 2568–2586 (2011).
- ⁴⁵⁷ ²²D. H. Werner, D.-H. Kwon, I.-C. Khoo, A. V. Kildishev, and V. M. Shalaev,
⁴⁵⁸ "Liquid crystal clad near-infrared metamaterials with tunable negative-zero-
⁴⁵⁹ positive refractive indices," *Opt. Express* **15**, 3342–3347 (2007).
- ⁴⁶⁰ ²³G. R. Keiser and P. Klarskov, "Terahertz field confinement in nonlinear meta-
⁴⁶¹ materials and near-field imaging," *Photonics* **6**, 22 (2019).
- ⁴⁶² ²⁴K. Fan, H. Y. Hwang, M. Liu, A. C. Strikwerda, A. Sternbach, J. Zhang,
⁴⁶³ X. Zhao, X. Zhang, K. A. Nelson, and R. D. Averitt, "Nonlinear terahertz meta-
⁴⁶⁴ materials via field-enhanced carrier dynamics in GaAs," *Phys. Rev. Lett.* **110**,
⁴⁶⁵ 217404 (2013).
- ⁴⁶⁶ ²⁵G. Allaire, "Homogenization and two-scale convergence," *SIAM J. Math. Anal.*
⁴⁶⁷ **23**, 1482–1518 (1992).
- ⁴⁶⁸ ²⁶S. Guenneau and F. Zolla, "Homogenization of three-dimensional finite pho-
⁴⁶⁹ tonic crystals," *J. Electromagnet. Waves Appl.* **14**, 529–530 (2000).
- ⁴⁷⁰ ²⁷S. Agrawal, R. Guo, D. Agrawal, and A. S. Bhalla, "Tunable BST:MgO dielec-
⁴⁷¹ tric composite by microwave sintering," *Ferroelectrics* **306**, 155–163 (2004).
- ⁴⁷² ²⁸M. A. H. Ansari, A. K. Jha, and M. J. Akhtar, "Design and application of the
⁴⁷³ CSRR-based planar sensor for noninvasive measurement of complex permittiv-
⁴⁷⁴ ity," *IEEE Sens. J.* **15**, 7181–7189 (2015).
- ²⁹L. D. Landau, J. Bell, M. Kearsley, L. Pitaevskii, E. Lifshitz, and J. Sykes, *475*
Electrodynamics of Continuous Media (Elsevier, 2013), Vol. 8. ⁴⁷⁶
- ³⁰K. Zhou, S. A. Bogg, R. Ramprasad, M. Aindow, C. Erkey, and S. P. Alpay, *477*
478 "Dielectric response and tunability of a dielectric-paraelectric composite," *479*
Appl. Phys. Lett. **93**, 102908 (2008).
- ³¹C. M. Krowne, M. Daniel, S. W. Kirchoefer, and J. A. Pond, "Anisotropic *480*
481 permittivity and attenuation extraction from propagation constant measure-*482*
483 ments using an anisotropic full-wave Green's function solver for coplanar fer-*484*
485 roelectric thin-film devices," *IEEE Trans. Microw. Theory Techn.* **50**, 537–548 *486*
487 (2002).
- ³²C. Geuzaine and J.-F. Remacle, "Gmsh: A 3-D finite element mesh generator *488*
489 with built-in pre- and post-processing facilities," *Int. J. Numer. Methods Eng.* *485*
79, 1309–1331 (2009). *486*
- ³³P. Dular, C. Geuzaine, F. Henrotte, and W. Legros, "A general environment *488*
489 for the treatment of discrete problems and its application to the finite element *490*
491 method," *IEEE Trans. Magn.* **34**, 3395–3398 (1998). *492*
- ³⁴P. R. Amestoy, I. S. Duff, J. Koster, and J.-Y. L'Excellent, "A fully asynchronous *491*
492 multifrontal solver using distributed dynamic scheduling," *SIAM J. Matrix *493**
Anal. Appl. **23**, 15–41 (2001).
- ³⁵G. Bouchitté and D. Felbacq, "Homogenization near resonances *494*
495 and artificial magnetism from dielectrics," *C. R. Math.* **339**, 377–382 *496*
497 (2004).
- ³⁶K. Cherednichenko and S. Cooper, "Homogenization of the system of high-*497*
498 contrast Maxwell equations," *Mathematika* **61**, 475–500 (2015).